AIP | Proceedings

Microbunching and coherent acceleration of electrons by subcycle laser pulses

Bernhard Rau, T. Tajima, and H. Hojo

Articles you may be interested in

Microbunching and Coherent Acceleration of Electrons by Subcycle Laser Pulses

Bernhard Rau, T. Tajima, and H. Hojo[†]

Physics Department
The University of Texas at Austin
Austin, Tx 78712

[†]Plasma Research Center
University of Tsukuba
Tsukuba 305, Japan

I. ABSTRACT

The pick up and acceleration of all plasma electrons irradiated by an intense, sub-cyclic laser pulse is demonstrated via analytical and numerical calculations. It is shown that the initial low emittance of the plasma electrons is conserved during the process of acceleration, leading to an extremely cold, bunched electron beam. Compression of the electron bunch along the longitudinal coordinate is naturally achieved due to the interaction of electrons and laser pulse. In this paper, we find the localized solutions to Maxwell's equations of a subcyclic laser pulse and use these to determine the acceleration of charged particles and we suggest future application for this acceleration mechanism as low energy particle injector and as electron source for coherent x-ray generation.

II. INTRODUCTION

The issue of particle bunching and pre-acceleration has always been a crucial point in accelerator physics. A low emittance source of tightly bunched particles is needed for almost all practical application of high energy particles. But while there is a great effort to replace the rf-driven accelerator schemes with high gra-

dient linear accelerators such as the laser wakefield accelerator, plasma wakefield accelerator, plasma beat wave accelerator, and others, less work has been done to replace electron guns with higher technology standards. Photo cathode work has been proposed and developed and recently, optical generation of pre-accelerated electron bunches has been proposed [1]. As beam loading and emittance issues become more important for a small scale high energy accelerator, researchers are in need of a cold source of bunched particles.

In this paper, we investigate the collective acceleration of plasma electrons by a properly shaped high intensity laser pulse. Those investigations are done analytically as well as with the help of a 1-$\frac{2}{2}$ PIC (particle in cell) code. We study the electron motion in the focal region of an ultrashort laser pulse and determine the electron bunch parameters such as emittance, bunch length, and beam energy.

In the next section, we analytically derive the 3-dimensional solution for the electromagnetic fields of a laser pulse of arbitrary length present inside the focal region. We use these fields to determine the acceleration of plasma electrons due to their interaction with a strong, ultrashort laser pulse in section IV. Section V will contain the analytical and numerical results for the acceleration parameters and in section VI, we will show applications of such electron bunches for high brilliance x-ray sources. We will conclude this paper in section VII.

III. 3-DIMENSIONAL FIELDS OF A SUBCYCLIC LASER PULSE

Electromagnetic waves of finite radial extent take a 3-dimensional expression. While other authors have derived expressions valid for long laser pulses [3, 2], their analysis fail to describe pulses whose envelope changes on a length scale comparable to the laser wavelength. Here, we derive solutions for a pulse of arbitrary length (and thus valid even for subcyclic pulses).

Assuming the x-polarized laser pulse to propagate along the z-direction far away from any boundaries, we can solve the vacuum wave equation for the x component of the electric field $E_x(r,z,t)$ in Fourier space $(\nabla^2 + k^2)\bar{E}_x(r,z;k = \omega/c) = 0$ to determine this field in a closed form expression

$$\bar{E}_x(r,z;k) = \frac{1}{2\pi} \int dp \int dq A(p,q;k) \exp[ik(px + qy + \sqrt{1 - p^2 - q^2}z)], \quad (1)$$

where the borders of integration must be chosen in a way that the resulting modes

will be bounded for all x, y, and z, i.e. p, q, and $\sqrt{1-p^2-q^2}$ must be real. The amplitude $A(p,q;k)$ is determined as

$$A(p,q;k) = \tilde{E}_0(k)\frac{k^2 w_0^2}{2}\exp[-k^2\frac{(p^2+q^2)w_0^2}{4}], \tag{2}$$

where we assumed $\tilde{E}_x(r,z=0;k) = \tilde{E}_0(k)\exp[-r^2/w_0^2]$. Choosing E_x to be cylindrically symmetric, the double integral in (1) can be reduced to an integral over the dimensionless variable $b = \sqrt{1-p^2-q^2}$. Assuming further that E_x has the same Fourier spectrum as its 1-dimensional counterpart, we find for the Fourier coefficients $\tilde{E}_0(k)$

$$\tilde{E}_0(k) = \frac{1}{\sqrt{2\pi}}\int_{-\infty}^{\infty} E_{1-D}(z=0,t)\exp[ikct]c\,dt$$

$$= \frac{E_0}{\sqrt{2\pi}}\int_{-\infty}^{\infty}\exp[-\frac{c^2t^2}{2\sigma^2}+ikct]\cos[-k_0ct]c\,dt$$

$$= E_0\sigma\exp[-\frac{k_0^2+k^2}{2}\sigma^2]\cosh[kk_0\sigma^2], \tag{3}$$

which, together with (1) and (2) gives the integral expression

$$E_x(r,z,t) = \frac{E_0 w_0^2\sigma}{2\sqrt{2\pi}}\exp[-\frac{k_0^2\sigma^2}{2}]\int_{-\infty}^{\infty}dk\,k^2\cosh[kk_0\sigma^2]\int_0^1 db\,b\,\times$$

$$\times\exp[-k^2(\frac{\sigma^2}{2}+\frac{w_0^2(1-b^2)}{4})+ik(zb-ct)]J_0(kr\sqrt{1-b^2}). \tag{4}$$

Here, w_0 is the spotsize of the laser pulse at the focal plane, k_0 is the k-number affiliated with the center frequency of the pulse, σ characterizes the pulse length, and E_0 is the pulse amplitude. With (4) and the assumption that E_y is 0 for all r, z, and t, we use the vacuum equations $\vec{\nabla}\cdot\vec{E} = 0$ and $-\partial\vec{B}/(c\,\partial t) = \vec{\nabla}\times\vec{E}$ to find the other components of the electric and magnetic fields as

$$E_z(x,y,z,t) = \frac{\partial}{\partial x}\left\{\frac{E_0 w_0^2\sigma}{2\sqrt{2\pi}}\exp[-\frac{k_0^2\sigma^2}{2}]\int_{-\infty}^{\infty}dk\,ik\cosh[kk_0\sigma^2]\int_0^1 db\,\times\right.$$

$$\left.\times\exp[-k^2(\frac{\sigma^2}{2}+\frac{w_0^2(1-b^2)}{4})+ik(zb-ct)]J_0(kr\sqrt{1-b^2})\right\}, \tag{5}$$

$$B_x(x,y,z,t) = \frac{\partial^2}{\partial x\,\partial y}\left\{\frac{E_0 w_0^2\sigma}{2\sqrt{2\pi}}\exp[-\frac{k_0^2\sigma^2}{2}]\int_{-\infty}^{\infty}dk\cosh[kk_0\sigma^2]\int_0^1 db\,\times\right.$$

$$\left.\times\exp[-k^2(\frac{\sigma^2}{2}+\frac{w_0^2(1-b^2)}{4})+ik(zb-ct)]J_0(kr\sqrt{1-b^2})\right\}, \tag{6}$$
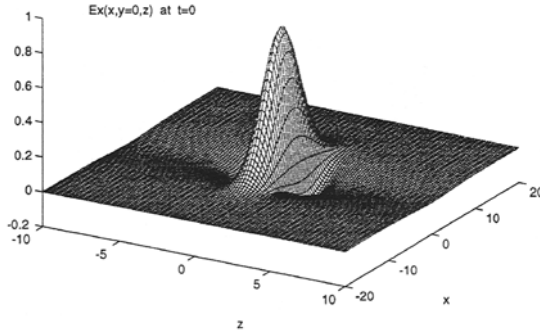
Figure 1: $E_x(x, y = 0, z, t = 0)$ [see Eq. (4)] for $k_0\sigma = 1$ and $w_0 = 5\sigma$. The units of the x and z axis are in σ.

$$B_y(x,y,z,t) = \frac{E_0 w_0^2 \sigma}{2\sqrt{2\pi}} \exp[-\frac{k_0^2\sigma^2}{2}] \int_{-\infty}^{\infty} dk \cosh[kk_0\sigma^2] \int_0^1 db \left\{ k^2 b^2 - \frac{\partial^2}{\partial x^2} \right\} \times$$

$$\times \exp[-k^2(\frac{\sigma^2}{2} + \frac{w_0^2(1-b^2)}{4}) + ik(zb - ct)]J_0(kr\sqrt{1-b^2}), \tag{7}$$

and

$$B_z(x,y,z,t) = \frac{\partial}{\partial y} \left\{ \frac{E_0 w_0^2 \sigma}{2\sqrt{2\pi}} \exp[-\frac{k_0^2\sigma^2}{2}] \int_{-\infty}^{\infty} dk \, ik \cosh[kk_0\sigma^2] \int_0^1 db \, b \times \right.$$

$$\left. \times \exp[-k^2(\frac{\sigma^2}{2} + \frac{w_0^2(1-b^2)}{4}) + ik(zb - ct)]J_0(kr\sqrt{1-b^2}) \right\}. \tag{8}$$

Equations (4) - (8) of course only represent one special localized solution to Maxwell's equations with the given frequency spectrum (3). A general solutions involves a super composition of different fields of that kind.

Other authors [3] have argued that the integral over b can be solved to a good approximation for large values of kw_0. While this is correct for mono-frequent (and therefore long) laser pulses, the approximation fails for short (large bandwidth) pulses as they always include frequencies with $kw_0 \ll 1$.

On axis, equations (5),(6), and (8) vanish so that we are left with E_x and B_y only. Furthermore, E_x can be expressed in closed form for $z = 0$ or for large values of z:

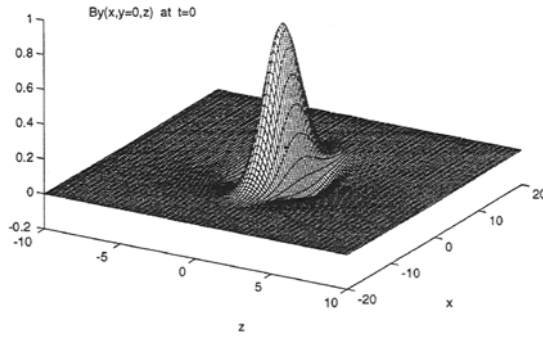$$E_y(r = 0,z,t) = E_z(r = 0,z,t) = B_x(r = 0,z,t) = B_z(r = 0,z,t) = 0, \tag{9}$$

769

Figure 2: $B_y(x, y = 0, z, t = 0)$ [see Eq. (7)] for $k_0\sigma = 1$ and $w_0 = 5\sigma$. The units of the x and z axis are in σ. For $w_0 \gg \sigma$, E_x (see Fig. 1) and B_y are very similar.

$$E_x(r = 0, z = 0, t) = E_0 \exp[-\frac{c^2 t^2}{2\sigma^2}] \cos[k_0 ct]$$
$$-\frac{E_0}{\sqrt{1+\rho^2}} \exp[-\frac{k_0^2 \sigma^2}{4(1+\rho^2)}] \exp[-\frac{c^2 t^2}{2\sigma^2(1+\rho^2)}] \cos[\frac{k_0 ct}{1+\rho^2}], \quad (10)$$

and

$$E_x(r = 0, |z| > \sigma \text{ and } |z| > \frac{w_0^2}{\sigma}, t) = \frac{E_0}{2} \exp[-\frac{(z-ct)^2}{2\sigma^2}] \times$$
$$\times \left\{ \exp[ik_0(z-ct)] \frac{z - ct - ik_0\sigma^2}{z - ct - ik_0\sigma^2 + z/\rho^2} + c.c. \right\}, \quad (11)$$

where we defined ρ as a ratio of transverse to longitudinal extent of the laser pulse to be $\rho^2 = w_0^2/(2\sigma^2)$. Equations (9) - (11) approach to correct limits for a 1-dimensional pulse of arbitrary length ($\rho \to \infty$) and for a 3-dimensional long pulse ($\rho \to 0$). Those fields will be used in the next section to determine the forces acting on charged particles around the focal point of a laser pulse.

770

IV. ELECTRON ACCELERATION BY SUBCYCLIC LASER PULSES

Assuming the fields (4)-(8) in the focal region of a large-spotsize pulse ($r \ll w_0, |z| \ll w_0, \rho = w_0/(\sqrt{2}\sigma) \gg 1$), we can use the 1-dimensional fields to determine the electron motion due to its interaction with the electromagnetic radiation. With

$$E_x(r,z,t) = B_y(r,z,t) \simeq E_0 \exp[-\frac{(z-ct)^2}{2\sigma^2}] \cos[k_0(z-ct)]$$
$$E_y(r,z,t) = E_z(r,z,t) = B_x(r,z,t) = B_z(r,z,t) \simeq 0, \tag{12}$$

we can use the z component of the relativistic Lorentz equation along with the time dependence of the power

$$m_0 c \frac{d\gamma}{dt} - m_0 c \frac{d(\gamma\beta_z)}{dt} = -e(\vec{\beta}\cdot\vec{E}) + e(E_z + \beta_x B_y - \beta_y B_x) \simeq 0 \tag{13}$$

to find the approximate constant $\gamma(1 - \beta_z)$ of the electron motion. The motion in the y direction is determined by the Lorentz force to become

$$m_0 c \frac{d(\gamma\beta_y)}{dt} = -e(E_y + \beta_z B_x - \beta_x B_z) \simeq 0. \tag{14}$$

Thus, inside the focal region we can neglect the motion along the y-direction. In this parameter regime, we can follow the analysis of Scheid & Hora [4]: For electron initially at rest ($\vec{v}_{init} = 0$), we integrate the x-component of the Lorentz equation with respect to the relative coordinate u to obtain the final normalized momentum in the x direction as

$$(\gamma\beta_x)_{final} = \frac{-e}{m_0 c} \int_{-\infty}^{+\infty} (E_x + \beta_y B_z - \beta_z B_y) dt$$
$$\simeq \frac{-e}{m_0 c} \int_{-\infty}^{+\infty} ((1-\beta_z)E_x) dt = \frac{e}{m_0 c^2} \int_{-\infty}^{+\infty} E_x \, du \equiv A. \tag{15}$$

Using (13), the final relativistic Lorentz factor γ_{final} can then be expressed in terms of the electric field E as $\gamma_{final} = 1 + A^2/2$. In particular, we find that a net energy gain due to the interaction of electrons and laser pulse is possible as long as A does not vanish, i.e. as long as the electric field E has a "zero-frequency" or DC component. For wave trains with more than a few oscillations, A vanishes in accordance with the Lawson-Woodward theorem [5].

771

Introducing the normalized vector potential $a_0 \equiv (eE_0)/(m_0 k_0 c^2)$, the electron gain for a wave packet of the form (4) - (8) becomes

$$\Delta E = a_0^2 m_0 c^2 \pi (k_0 \sigma)^2 \exp[-(k_0 \sigma)^2]. \tag{16}$$

Maximum gain for a given field amplitude E_0 is thus obtained for $k_0 \sigma = 1$, which entails the optimum pulse width being shorter than one wavelength (see Fig. 1). Such pulses have been successfully generated in the microwave [6], far infrared [7], and even in the femtosecond regime [8]. However, their amplification to higher intensities proves to be complicated [9] as the gain media normally used for amplification do not support such large bandwidths.

In the regime of $\beta_y^2 \ll \beta_x^2 + \beta_z^2$ (i.e. inside the focal region of a loose focus), we can find the angle φ between final electron motion and z axis to be $\varphi = \arctan[\beta_x/\beta_z]$. But, since $\gamma = 1 + A^2/2$ and $\gamma \beta_x = A$, φ is determined by

$$\varphi = \arctan \frac{2}{A} = \arctan \sqrt{\frac{2}{\gamma - 1}}. \tag{17}$$

Hence, we expect the electrons to be ejected at an angle which depends on the electron energy. For electrons with kinetic energies of or exceeding 1MeV, the main part of their momentum however will be along the z axis, while for highly energetic particles ($\gamma \gg 1$), the angle approaches $\varphi \simeq \sqrt{2}\gamma^{-1/2}$.

So far, we have only addressed the pickup of a single electron by a subcyclic laser pulse in vacuum. In the next section, we will address the coherent acceleration of all the plasma electrons on the spot using those electromagnetic pulses. The relevant injector properties will be discussed.

V. MICROBUNCHING AND COHERENT ELECTRON ACCELERATION

For the generation of tightly bunched electron pulses, we propose to inject a subcyclic laser pulse into a thin layer of plasma. While the heavy ions remain inertial during such a short time scale, the plasma electrons will be expelled from the initial plasma region and accelerated. Since this acceleration to relativistic velocities takes place on a time scale of the pulse length, space charge forces between the electrons are practically absent. However, an ambipolar electrostatic field E_{amb} will be generated due to the separation of plasma electrons and

772

ions which requires the laser pulse to be powerful enough such that the accelerated electrons overcome this repulsive potential. Using (16), this condition can be rewritten as $\Delta E > \int_0^\infty eE_{amb}(z,t)\,dz$. The ambipolar field however will decay both along the longitudinal axis (due to a finite spotsize) as well as in time (due to the electron response of the plasma remaining outside the transverse focal region), so that we can find the lower limit for the laser pulse intensity to be $m_0 c^2 \pi (k_0\sigma)^2 a_0^2 \exp[-(k_0\sigma)^2] > \int_0^{L_p} 4\pi n_0 e^2 z\,dz$, or, assuming $k_0\sigma = 1$,

$$a_0^2 > \frac{\exp[1]}{2\pi}\left(\frac{L_p}{c/\omega_p}\right)^2. \tag{18}$$

Here n_0 is the electron density of the initial plasma, L_p is its longitudinal extent, and ω_p is the plasma frequency. Eq. (18) shows that even plasma length of the order $O(c/\omega_p)$ require relativistically strong field amplitudes ($a_0 > 1$). Very much the same way, we can estimate the number of electrons accelerated per shot:

$$N/S = n_0 L_p < a_0^2/(2r_e L_p \exp[1]), \tag{19}$$

where $r_e = e^2/(m_0 c^2)$ and S is the transverse area over which the intensity of the wave packet is nearly constant (typically $O(1/k_0^2)$). For plasma lengths of the order of 1 μm, the upper limit for the number of electrons per unit area is $N/S[\text{mm}^{-2}] < a_0^2 \cdot O(10^{13})$, which even for moderate values of a_0 seems to be sufficient to fulfill the needs of particles per bunch in modern accelerators/injectors.

Finally, we can estimate the emittance of the electron bunch by calculating the initial longitudinal and transverse emittance. The normalized emittance ε_N is defined as the product of spatial and normalized momentum spread by $\varepsilon_N = \sqrt{<\Delta z^2><\Delta p_z^2> - <\Delta z\Delta p_z>^2}/(m_0 c)$, with the usual definition of the variance $<\Delta A^2> = <A^2> - <A>^2$ and $<A> = \sum_{i=1}^N A_i/N$. For a plasma of longitudinal extend L_p in thermal equilibrium with a plasma electron temperature T_e, we find $<\Delta z^2> = L_p^2/12$ and $<\Delta p_z^2> = m_0 T_e$ (and $<\Delta x\Delta p_x>^2 = 0$), so that the initial longitudinal emittance becomes

$$\varepsilon_{N,long}^{init} = \sqrt{\frac{L_p^2}{12}\frac{T_e}{m_0 c^2}}, \tag{20}$$

or about $4.0\cdot 10^{-4} L_p[\mu m]\sqrt{T_e[\text{eV}]}$ mm mrad. (Or $\varepsilon_{N,long}^{init} \approx 6.9\cdot 10^{-10} L_p[\mu m]$ $\sqrt{T_e[\text{eV}]}$ eV-sec when we express $\varepsilon_{N,long}^{init}$ in eV-sec.) The initial transverse emittance for a circular area S becomes with $<\Delta r^2> = S/(2\pi)$ and $<\Delta p_r^2> = 2m_0 T_e$

$$\varepsilon_{N,trans}^{init} = \sqrt{\frac{S}{\pi}\frac{T_e}{m_0 c^2}}, \tag{21}$$
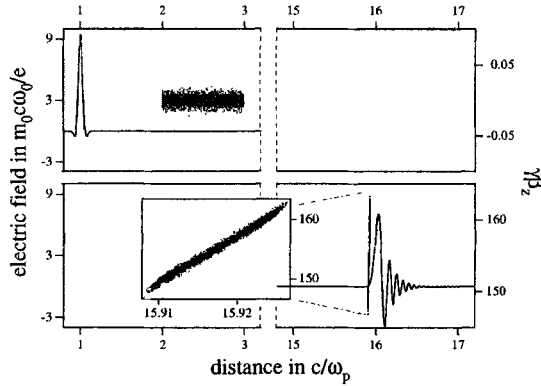
Figure 3: Initial and final transversal electric field and phase space for $L_p = 1c/\omega_p$, $\omega_0/\omega_p = 30$, and $a_0 = 10$. Inset: blow up of the final longitudinal phase space

or ca. $7.9 \cdot 10^{-1}\sqrt{S[\text{mm}^2]T_e[\text{eV}]}$ mm mrad. With the above threshold ionization of atoms in the ultrashort pulse regime, the expected electron temperature T_e is only a few eV. Thus for a plasma volume $L_p \times S \sim 1\mu\text{m} \times 3 \cdot 10^{-4}\text{mm}^2$, $\varepsilon_{N,long}^{init}$ is expected to be of the order $1 \cdot 10^{-3}$ mm mrad and $\varepsilon_{N,trans}^{init}$ of the order of $1.5 \cdot 10^{-2}$ mm mrad.

As mentioned above, space charge effects are practically absent due to the rapid acceleration of the electrons to relativistic velocities and do therefore not increase the emittances. However, the three dimensional nature of the electromagnetic fields may lead to unstable regions of betatron oscillations that will affect the electron momentum spread so that the final emittance might grow in the process of acceleration. Additional growth due to the transverse accelerating structure is possible, but both growth rates can be minimized for a geometry with a loose focus ($\rho = w_0/(\sqrt{2}\sigma) \gg 1$).

We simulated the interaction of a subcyclic laser pulse with a plasma slab of finite extent using a $1 - \frac{2}{2}$ dimensional PIC code. The laser pulse was initialized in the vacuum region outside the plasma and evolved into the layer (see Fig. 2). After its propagation through the plasma layer, the pulse enters the vacuum region behind the slab, carrying with it the expelled electrons, while the heavy ions are left behind. For this simulation, we used a $2^{11}\Delta$ large simulation box with vacuum boundary conditions. About 8000 macro particles made up the quasi neu-
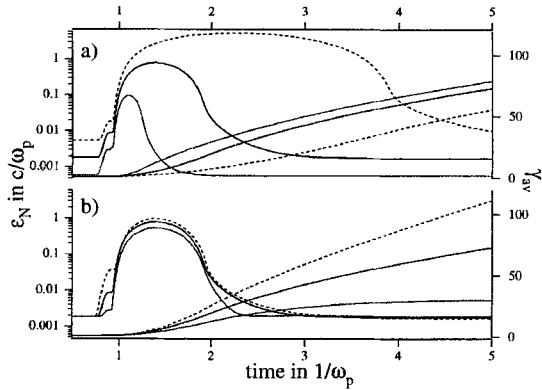
Figure 4: Normalized phase space volume and γ_{av} as a function of time for a) $a_0 = 10$, $L_p = 1/3$(dotted), 1(solid), and 3(dashed line) c/ω_p and b) $a_0 = 5$(dotted), 10(solid), and 20(dashed line) $L_p = 1$ c/ω_p. The initial growth of the phase space volume is due to fact that the electron are not accelerated simultaneously. Once The pulse passes the plasma slab, all the electron experience the acceleration force and the longitudinal phase space volume decays to its initial value.

tral plasma initially in thermal equilibrium with an electron temperature varied between 1 and 1,000 eV. Since the ambipolar field E_{amb} does no decay in a 1-D simulation, we stopped the run at a point where the laser pulse just passed the electrons. As mentioned above, multidimensional effects let the potential decrease with both increasing distance and time. Such effects where manually implemented into the 1-D code but did not lead to any qualitatively different results. A rigorous investigation however requires the help of a 2 or 3-D simulation and has not been conducted yet.

Due to the interaction with the laser pulse, the expelled electron bunch becomes compressed along its longitudinal axis (see inset of Fig. 2) and spread in momentum space. The normalized longitudinal emittance ε_N^{long} however remains approximately constant (see Fig. 3 (a) and (b)). Typically, a spatial compression of a factor 100 is naturally achieved within the laser-electron interaction. This seems to be due to the fact that the pulse loses its "zero-frequency" or DC component energy to the electrons. Particles in the trailing part of the beam extract this energy more efficiently, since the pulse, traveling with the speed of light, passes

the bunch from the behind and supplies undepleted energy to those electrons being located in the back of the bunch. Thus, those electrons are accelerated forward until they line up with the leading part. Ideally, all the electrons gather in a plane in the reference frame of the particle bunch and coherently extract the pulse energy.

The parameters used for the results displayed in Fig. 2 are $a_0 = 10$, $\omega_0/\omega_p = 30$, and $L_p = c/\omega_p$. From Eq. (16), we would expect an average relativistic Lorentz factor $\gamma_{av}^{pred.} \simeq 116.6$. Comparing this with the simulation (see inset of Fig. 2), the average Lorentz factor is well above 150. This finds its explanation in the fact that the laser pulse group velocity slows down as the particle-wave interaction takes place and thus extents the time for the energy exchange. In particular, the phase velocity of the DC component slows down while the component itself becomes depleted, leading to a chirp of the laser pulse.

VI. APPLICATIONS OF ELECTRON MICROBUNCHES

The parameters found in the previous section can now be evaluated in few of possible future applications of this particle accelerating mechanism. So could a Ti:Sapphire laser capable of generating subcyclic pulses and operating at an intensity of about $3.6 \cdot 10^{18} \mathrm{W}/\mathrm{cm}^2$ ($a_0 \approx 1.3$, see Fig.4 for similar setup) be used as a table top particle injector. From the irradiation of a plasma layer of about 1-2 μm thickness at a plasma electron density of about $2 \cdot 10^{18}/\mathrm{cm}^3$ we could expect about $3 \cdot 10^{12}$ electrons$/\mathrm{mm}^2$ at a kinetic energy of 1 MeV. The longitudinal emittance $\varepsilon_{N,long}$ should be as low as $2 \cdot 10^{-3}$ mm mrad (assuming a temperature of 10 eV). The initial transverse emittance $\varepsilon_{N,trans}^{init}$ is then (assuming the irradiated area of constant intensity to be about $c^2/\omega_p^2 \approx 14\mu\mathrm{m}^2$) ca. $9 \cdot 10^{-3}$ mm mrad.

Another future application of this acceleration mechanism might be the use as a bright x-ray source. Since the synchrotron radiation of bunched charged particles becomes enhanced by a factor of N_b, the number of particles per bunch, if the wavelength λ of the synchrotron radiation is less than the bunch length λ_b [11], we can expect highly coherent and enhanced radiation from bunches with a bunch length λ_b smaller than the critical wavelength $\lambda_c = (4\pi m_0 c^2)/(3\gamma^2 eB)$, where B is the magnetic field strength of the synchrotron magnets. Since the longitudinal particle bunching is small to begin with ($O(c/\omega_p)$) and becomes compressed by a factor of about 100 in the process of acceleration (see Fig. 2), we might be able to achieve electron bunch lengths of the order of Å's. To estimate the brilliance
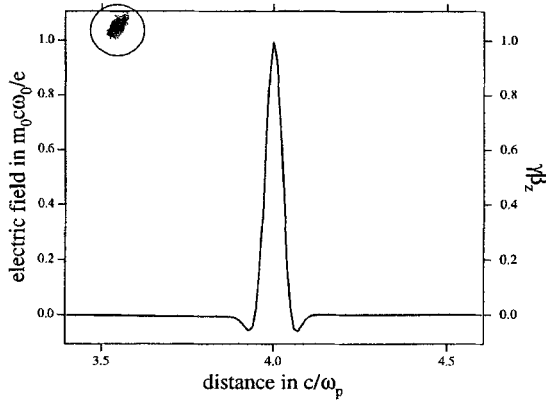
776

Figure 5: Final electric field and phase space for $a_0 = 1$. The plasma was initialized as shown in Fig. 2 (between $2 \leq \frac{c}{\omega_p} \leq 3$). The particles inside the circle represent the entire final phase space.

b of such a particle bunch, we use the frequency and angular dependence of the radiated energy E_{rad} [12] on axis for a single electron

$$\frac{d^2 E_{rad}}{d\omega \, d\Omega}\bigg|_{\text{on axis}} = \frac{3e^2\gamma^2}{4\pi^2 c} \left(\frac{\omega}{\omega_c}\right)^2 K_{2/3}^2 \left(\frac{\omega}{2\omega_c}\right) \tag{22}$$

and express the number of photons per electron radiated in the frequency bandwidth $\Delta\omega/\omega$ as

$$\frac{d \text{ \# of photons}}{d\Omega} = \frac{3\alpha\gamma^2}{4\pi^2} \left(\frac{\omega}{\omega_c}\right)^2 K_{2/3}^2 \left(\frac{\omega}{2\omega_c}\right) \frac{\Delta\omega}{\omega} , \tag{23}$$

which leads to a spectral brilliance of

$$b = 10^{-9} \frac{3\alpha\gamma^2}{4\pi^2} \left(\frac{\omega}{\omega_c}\right)^2 K_{2/3}^2 \left(\frac{\omega}{2\omega_c}\right) \rho[\text{mm}^{-2}] \nu[\text{s}^{-1}] . \tag{24}$$

Here b is the brilliance in $\frac{\text{\# of photons}}{\text{sec. mrad}^2 \, \text{mm}^2 \, 0.1\% \frac{\Delta\omega}{\omega}}$, $K_{2/3}$ is the modified Bessel function of the second kind, $\alpha \simeq 1/137$ is the fine structure constant, ρ is the particle density N/S for the incoherent and N^2/S for the coherent synchrotron radiation, ν is the repetition rate (for the average brilliance) or the inverse radiation time for a

777

single bunch ($\approx c/\lambda_b$ for the peak brilliance), and $\omega_c = 2\pi c/\lambda_c$ is the critical frequency. Due to the angular divergence of the photon packet, the spectral brilliance at the target however will be smaller by a factor $(r_0\gamma/(r_0\gamma + d))^2$ with r_0 being the radius of the irradiated area and d the distance between metallic film and target.

Using a metallic film ($n_0 \sim O(10^{23}/\text{cm}^3)$) of several ten atomic layers for the initial plasma slab, we could produce bunch lengths in or even below the angstrom regime, which would lead to the coherent production of x-ray radiation. Of particular interest is the generation of soft x-ray radiation at the "water-window" spectral region ($\lambda = 2.3 - 4.4$ nm) [13]. Assuming the electron bunch production from a $L_p = 0.1c/\omega_p$ thick metal film at $n_0 = 10^{23}/\text{cm}^3$ by this mechanism, the final bunch length is expected to be in the angstrom regime. Assuming further that the bunch could be accelerated to electrons energies of 2 GeV while preserving this bunch length, a magnetic field of $B = 0.24$T would be sufficient to generate synchrotron radiation with a critical wavelength λ_c of 2nm. With $N/S \simeq 1.68 \cdot 10^{14}/\text{mm}^2$ and $S \simeq 10^{-3}\text{mm}^2$, Eq. (24) leads to an average brilliance of coherent synchrotron radiation at $\omega \approx \omega_c$ exceeding $3 \cdot 10^{21} \dfrac{\text{photons}}{\text{sec. mrad}^2\,\text{mm}^2\,0.1\%\frac{\Delta\omega}{\omega}}$

at a repetition rate ν of 10Hz. Assuming the bunch length λ_b to be 1 Å, the peak intensity at $\omega \approx \omega_c$ would be greater than $10^{39} \dfrac{\text{photons}}{\text{sec. mrad}^2\,\text{mm}^2\,0.1\%\frac{\Delta\omega}{\omega}}$. The value for the average brilliance would be of the same order as the one proposed for the LINAC coherent light source at the Stanford Linear Accelerator Center [14] and the one proposed for TESLA-FEL at DESY, Hamburg [15], while the value for the peak brilliance would exceed those proposed for SLAC and DESY by several orders of magnitude.

Extreme short electron bunches created by this mechanism might also be of interest for exciting a wakefield in a crystal. Short electron bunch lengths and high electron densities within the bunch may be used to resonantly excite electrostatic waves along a nano [17] or meso hole structure [18] of a crystal. In [17], pores of radii of several lattice spacings are etched through finite volumes of a single crystal. Electron scattering off valence- and conduction-band electrons (and nuclei) is drastically reduced along those channels while a coherent wakefield structure over many lattice spacings is still possible. The length scale of the acceleration structure ($\sim c/\omega_p$) along a nanohole (background electron density $\sim 10^{24}/\text{cm}^3$) is about ≈ 50 Åand thus of the same order as the hole radius. Since the particle density of the driving beam should be on the order of (or even higher than) the ambient electron density, the desired electron bunches could be produced using the a metallic film as discussed above. In this case, the thickness of the film should be several hundreds Åwhich would require a laser pulse $a_0 > 3$ (see Eq.(18)). Since

the transverse dimension of the electron bunch is expected to be much larger than the nanohole diameter, a honeycomb-like hole structure in the material would be necessary to reduce the number of "unused" electrons in the bunch. For the length scale of the wakefield wavelength to be of the order of the transverse dimension of a microhole, a material with an ambient plasma electron density of about $10^{20}/cm^3$ could be used. Here, the electron bunch could be produced from a $\sim 5\mu m$ thin plasma layer like the one mentioned before in this section. Once again, Eq. (18) requires a laser strength for this case of $a_0 > 2$.

The energy gain of the electrons due to their acceleration from rest by sub-cyclic pulses scales was found to scale proportional to a_0^2, as could be expected from (16). Comparing this to the energy gain of electrons in the laser wakefield accelerator scheme (which is proportional to $\omega_0^2/\omega_p^2)a_0^2$, [10]), we may not suggest this mechanism to be used for acceleration of particles to very high energies. Furthermore, the energy gain for highly relativistic particles per stage is only proportional to $a_0^{2/3}$ as will be shown in the following: The equation of motion for the z component of a highly relativistic particle ($\gamma \gg 1$, $\beta_z \approx 1$) becomes

$$m_0c\frac{d\gamma}{dt} \approx m_0c\frac{d\gamma\beta_z}{dt} = -e(E_z + \beta_xB_y - \beta_yB_x) \approx -e\beta_xE_x \approx -e\sqrt{2}\gamma^{-1/2}E_x , \quad (25)$$

since $\beta_x/\beta_z = \sqrt{2/(\gamma-1)}$. Time integrating this, we find $\gamma(t + \Delta t) = [\gamma(t)^{(3/2)} + (3E_x\Delta t)/(\sqrt{2}m_0c)]^{(2/3)}$. Since the interaction length $c\Delta t$ is limited to about twice the vacuum diffraction length Z_R, iteration over n acceleration stages leads to a γ-factor of

$$\gamma(n\Delta t) \simeq \left(\gamma(0)^{\frac{3}{2}} + n3\sqrt{2}a_0k_0Z_R\right)^{2/3} \simeq \left(n3\sqrt{2}a_0k_0Z_R\right)^{2/3} \quad (26)$$

Assuming the "long pulse" diffraction length $Z_R = k_0w_0^2$, (26) can be rewritten as $\gamma \approx (n3\sqrt{2}a_0k_0^2w_0^2)^{2/3}$ in the highly relativistic limit. [1] Thus, a multi-stage electron collider at 1 TeV with a center wavelength $\lambda_0 \simeq 1\mu m$, $a_0 \simeq 1$, and $w_0 \simeq 10\lambda_0$ (which amounts to a laser power of about 13 PW per stage) would then require about 160,000 of such stages.

Finally, we should mention that this acceleration mechanism might have astrophysical applications as well: Magnetic field lines wrapped tightly around rotating

---

[1]This result is somewhat misleading as one could conclude that the energy gain can be made infinitely big just by increasing the spotsize w_0 while keeping the laser power $P \propto a_0^2w_0^2$ constant. However, for equation (26) we assumed that the electron does not dephase significantly with the pulse center during the interaction. This becomes wrong in the 1-dimensional limit ($w_0 \to \infty$) and (26) must be replaced by $\gamma(t + \Delta t) \approx (2 + \pi a_0^2/\exp[1])/(2\gamma(t)(1 - \beta_z))$ [4].

discs, as it is believed to be the case for binary stars or super-massive black holes [16], may generate strong, whip-like motions of Alfvén waves due to magnetic reconnection. Those Alfvén waves can convert into subcyclic electromagnetic pulses which then causes particle acceleration and γ-bursts.

VII. CONCLUSION

In conclusion, we proposed a new method for the generation of cold and tightly bunched electrons. Electron bunches produced by the irradiation of thin plasma layers with subcyclic laser pulses are expected to have extremely low emittance while still supporting a sufficient number of electrons per bunch to meet future accelerator requirements. The longitudinal extent of those bunches can be so small that highly intense coherent synchrotron radiation at x-ray frequencies could be generated. In addition to this, these particle bunches could be used as drivers for a crystal plasma wakefield accelerator. We also pointed out that this acceleration mechanism could be of astrophysical interest as well.

ACKNOWLEDGMENTS

References

[1] D. Umstadter, J. K. Kim, and E. Dodd, Phys. Rev. Lett. **76**, 2073 (1996).

[2] M. Lax, W. H. Louisell, and W. B. McKnight, Phys. Rev. A **11**, 1365 (1975); L. W. Davis, Phys. Rev. A **19**, 1177 (1979).

[3] G. P. Agrawal and D. N. Pattanayak, J. Opt. Soc. **69**, 575 (1979); L. Cicchitelli, H. Hora, and R. Postle, Phys. Rev. A **41**, 3727, (1990).

[4] W. Scheid and H. Hora, Laser Part. Beams **7**, 315 (1989).

[5] J. D. Lawson, IEEE Trans. Nucl. Sc. **NS-26**, 4217 (1979), P. M. Woodward, Journal IEE **93**, Part III A, 1554 (1947).

[6] C. W. Domier, N. C. Luhmann, A. E. Chou, W-M. Zhang, and A. J. Romanowsky, Rev. Sci. Instrum. **66**, 339 (1995).

[7] C. Raman, C. W. S. Conover, C. I. Sukenik, and P. H. Bucksbaum, Phys. Rev. Lett. **76**, 2436 (1996).

[8] A. Bonvalet, M. Joffre, J. L. Martin, A. Migus, Appl. Phys. Lett. **67**, 2907 (1995).

[9] G. Mourou and C. P. J. Barty, private communication.

[10] T. Tajima and J. M. Dawson, Phys. Rev. Lett. **43**, 267 (1979), E. Esarey and M. Pilloff, AIP Conf. Proc. **335**, 574 (1995).

[11] J. K. Koga, T. Tajima, and Y. Kishimoto, "The Future of Accelerator Physics", ed. T. Tajima (AIP Conf. Proc., NY 1996), pg. 424, F. C. Michel, Phys. Rev. Lett. **48**, 580 (1982).

[12] J. D. Jackson, "Classical Electrodynamics", 2nd ed., J. Wiley & Sons (1975).

[13] I. C. E. Turcu et. al., J. Appl. Phys. **73**, 8081 (1993), R. A. London, M. D. Rosen, and J. E. Trebes, Appl. Opt. **15**, 3397 (1989).

[14] G. Materlik, Phys. Bl. **51**, 286 (1995).

[15] J. Roßbach, Phys. Bl. **51**, 283 (1995).

[16] C. A. Haswell, T. Tajima, J.-I. Sakai, Astrophys. J. **401**, 495 (1992).

[17] B. Newberger, T. Tajima, F. R. Huson, W. Mackay, B. C. Convington, J. R. Payne, Z. G. Zou, N. K. Mahale, and S. Ohnuma, "Proc. of the 1989 IEEE Particle Accelerator Conference", ed. F. Bennett and J. Kopta, pg. 630 (1989).

[18] B. Meerson and T. Tajima, Opt. Comm **86**, 283 (1991).